CHAPTER – 7

EFFECT OF STORAGE ON THE OIL BODIES, OLEOSIN – PROTEIN AND DNA

7.1. INTRODUCTION

7.1.1. Oil body and its synthesis

Seed oil is stored as lipid droplets; considered to be subcellular structures in cytoplasm, called oil bodies. Circular oil bodies or even ovoid oil bodies vary in diameter in size from one species to another species (range from 0.5µm to 2.5µm) (Huang, 1992; Tzen et al., 1993; Wang et al., 2012). However there are species that have oil body size few diameters lager than 2.5 µm as seen in Pongamia and Soybean. Triacylglycerols (TAG) are the chief constituents of the oil bodies which are enclosed by phospholipid monolayer (PL) which are in turn embedded with integral membrane protein called oleosin (Huang, 1992; Tzen et al., 1993; Tzen,2012). Many isoforms of oleosins have been identified. Besides oleosin, caleosin and steroleosin are the other two important integral membrane proteins (Chen et al., 1999; Tzen, 2012). The genome of model plant *Arabidopsis* has 16 oleosin genes of which 5 are seed specific (Shimada et al., 2008). The oil bodies within cytoplasm are maintained as discrete structures by these integral membrane proteins. In studies conducted in soybean, knocking down of the gene responsible of oleosin formation leads to the development of giant oil bodies (Schmidt and Herman, 2008; Shimada et al., 2018). Oil body biogenesis is comprised of three major parts: it starts with the biosynthesis of fatty acids (FAs) and then assembly of TAG takes place and finally there is a formation of oil bodies. In developing seeds, the oil body formation is regulated by multiple steps (Song et al., 2017).

7.1.2. Fatty acid synthesis

Fatty acids are synthesized in plastids of the seed through *de novo* pathways. Pyruvate being a precursor for fatty acid synthesis, entry of pyruvate into plastid from cytoplasm may come either through passive mechanism or by unknown translocator (Hajduch et al., 2011; Wheeler et al., 2016). At times phosphoenol pyruvate also gets

imported into the plastid via translocator where upon pyruvate is formed via pyruvate kinase present in plastid. Malate as well gets imported with the resultant effect of being converted to pyruvate (Hajduch et al., 2011; Gerrard Wheeler et al., 2016). By the catalytic action of acetyl-CoA carboxylase and fatty acid synthase, pyruvate present in plastid is converted to 16:0 ACP, 18:0 ACP and 18:1 ACP (acyl carrier protein) through a cascade reactions (Chapman and Ohlrogge, 2012). Growing FA chain attached covalently to the acyl carrier protein gains two carbon fragments during the process. Two acyl-ACP thioesterases convert 16:0 ACP, 18:0 ACP and 18:1 ACP into respective fatty acids (Ohlrogge and Browse, 1995; Chapman and Ohlrogge, 2012). At the chloroplast outer envelope, these nascent fatty acids are activated to 16:0 CoA, 18:0 CoA and 18:1 CoA and later transferred to endoplasmic reticulum (ER) for the TAG formation. Majority of the lipid-rich seeds contain C16 or C18 saturated and unsaturated fatty acids as storage (Song et al., 2017).

7.1.3. Triacylglycerol (TAG) assembly

Transferring of fatty acids from acyl-CoA to the glycerol-3-phosphate at sn-1 and sn-2 position yields phosphatidic acid (PA) as central metabolite in TAG assembly. Glycerol-3-phosphate acyltransferase (GPAT) and lysophosphatidic acid acyl transferase (LPAAT) are the enzymes responsible for the synthesis of phosphatidic acid. Dephosphorylation of phosphatidic acids results in the formation of diacylglycerol (DAG). Diacylglycerolacyltransferase (DGAT) transfers the third fatty acid to sn-3 position. Phosphatidylcholine (PC) is formed from DAG which also can be utilized for the synthesis of TAG (Bates et al., 2013; Xu and Shanklin, 2016). DGAT1 and DGAT2 are the major diacylglycerol acyltransferases present in endoplasmic reticulum which catalyses the conversion of DAG into TAG (Bates et al., 2013).

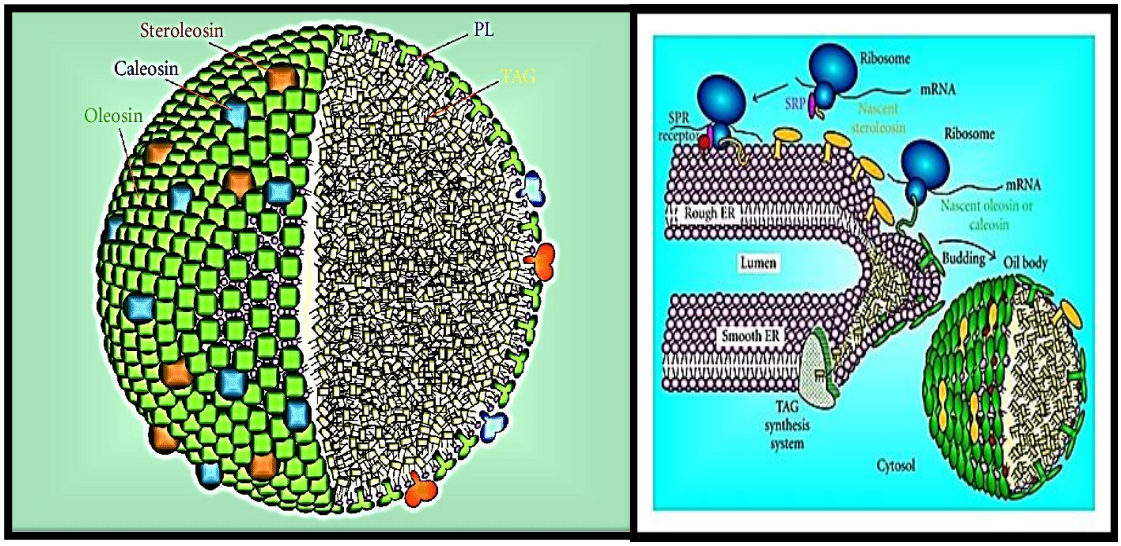

Figure 7.1: A structural model of an oil body assembly with three types of integral oil-body proteins and synthesis of oil bodies in ER (Tzen, 2012).

The synthesized TAG gets packed into circular oil bodies. Oil bodies have TAG as their core constituent which is surrounded by a layer of phospholipids with abundant oleosin proteins embedded into phospholipids. Molecular weight of these amphipathic proteins vary from ~15 to 30 kDa (Chapman et al., 2012). Other integral membrane proteins such as caleosin and steroleosin are also present in smaller amount. Oleosins are inserted co-translationally into ER in order to associate with phospholipids (Hsieh and Huang, 2004; Shimada and Hara-Nishimura, 2010; Tzen, 2012; Chapman et al., 2012). Fully synthesized oil bodies that contain TAG as core with over lay of phospholipids embedded with oleosin eventually bud off from ER to be accumulated in cytoplasm (Song et al., 2017). Oleosin is composed of a central lipophilic anchoring domain along with N-terminal amphipathic and C-terminal amphipathic domain (Huang, 1992; Tzen et al., 1993; Tzen, 2012). Around 30% of the amino acids of oleosin are located in the matrix of TAG and 20% are immersed into the layer of phospholipids and remaining 50% are exposed to the cytosol (Tzen et al., 1993). The primary function of the oleosins is to stabilize the oil bodies thus help to prevent coalescence of oil bodies by rendering steric hindrance and electronegative repulsion (Tzen et al., 1992; Tzen and Huang, 1998). Oil bodies' structural integrity within cytoplasm is maintained by these oleosins (Tzen 2012). The small oil bodies only contain oleosin as determined by immune-confocal laser scanning microscopy. The oil seeds that contain large oil bodies may lack oleosins. Under this situation LDAP1 and

LDAP2 – the lipid-associated proteins does the function of oleosin in stabilizing the large oil bodies (Horn et al., 2013).

The central domain is composed of 75 uncharged residues of amino acids. It is hydrophobic in nature and rich in aliphatic amino acids, glycine, alanine, leucine, isoleucine and valine (Li et al., 2002; Capuano et al., 2007). This domain forms a hairpin structure that penetrates the phospholipids present on the surface of the oil bodies into matrix. At the centre of this hydrophobic structure there is a formation of "Proline knot" which arises from the interaction of three proline residues and one serine residue (Hsieh and Huang, 2004) (Figure 7.2). N and C terminal domains are hydrophilic in nature (Huang, 1996). Approximately, 30 residues away from the hydrophobic domain, the C-terminal forms an amphipathic alpha helical structure horizontally with charged groups of phospholipids composed of choline and phosphate groups on the surface of the oil bodies (Tzen et al., 1992; Hsieh and Huang, 2004). The N – terminal is composed of several short peptides of glycine residues which are not conserved. Thus oleosins are generally Gly-rich proteins.

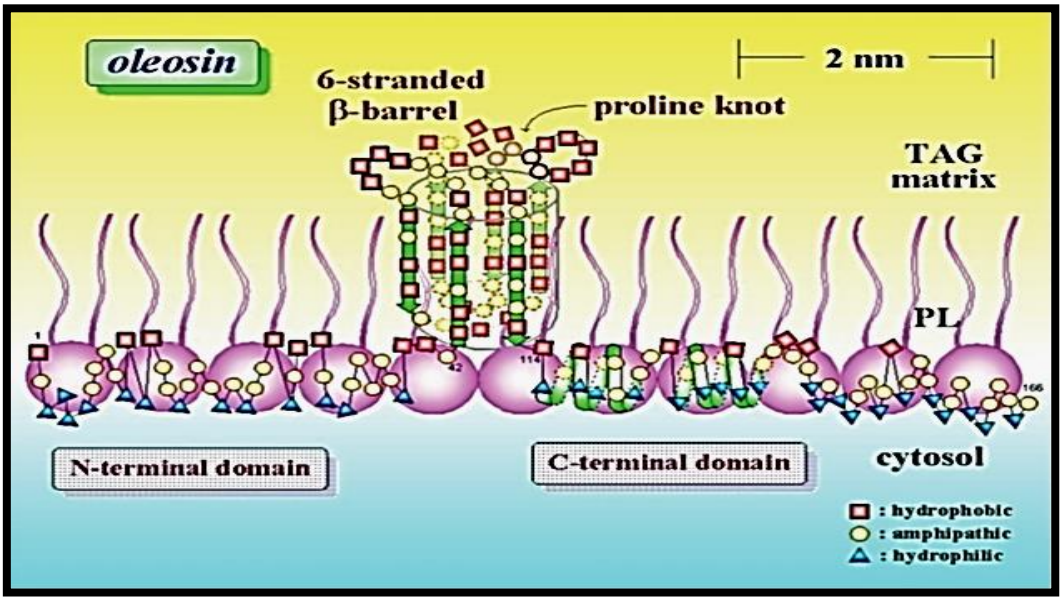

Figure 7.2: The secondary structure of oleosin (Tzen et al., 2003).

7.1.4. Isoforms of oleosin

Oleosin is found mainly in two forms H- and L- (high and low molecular weight) oleosins (Tzen et al., 1990). At the C-terminal domain of H oleosin an insertion of 18 residues leads to the formation of high molecular weight oleosin protein (Tai et al., 2002; Simkin et al., 2006; Chua et al., 2008). Physiological and molecular

significance of these two isoforms of oleosin in oil bodies not clearly understood (Tzen, 2012).

7.1.5. Characterization of *J. curcas* oleosin

In *silico* analysis by Popluechai et al., (2011) revealed that the three types of *J. curcas* oleosins namely *JcOleosin 1, JcOleosin 2, JcOleosin 3* are present within the seeds. All contain a hydrophobic region of 82, 83 and 79 amino acids, respectively. Proline knot consisting of serine residue at the centre (PXXXXXSPXXXP) is common to all three *J. curcas* oleosins. The large central region is mainly characterized by negative value indicating the presence of hydrophobicity. Insertion of an additional 18 residues in *JcOleosin 1* and *JcOleosin 2* qualifies them as H – form oleosins while *JcOleosin3* is an L-form oleosin. Image analysis of gel and densitometric scanning indicated that among all the other extracted oil body proteins 87% constituted oleosin proteins (Popluechai et al., 2011).

7.1.6. DNA and RNA integrity and damage

ROS, besides getting localized in cytoplasm and other organelles also find their way to the nuclei (Ashtamker et al., 2007). Their damaging effect on DNA causes viability loss in stored seed. Seeds kept for storage or artificial aging are easily prone to oxidative attack. Hydroxyl radical being most detrimental in nature is highly associated with the loss of DNA integrity and further DNA damage by catalysing the oxidation of nitrogenous bases, i.e. pyrimidines and purines (Bray and West, 2005; Moller et al., 2007). Significant deleterious changes were observed in nucleic acids which culminated in DNA fragmentation in aging seeds (Osborne, 2000; Kranner et al., 2011). The transcriptome wide mapping of pea seeds subjected to controlled deterioration has revealed the triggering of the genes responsible for DNA degradation and fragmentation eventually leading to programmed cell death (PCD) in aging pea seeds(Chen et al., 2013).

The integrity of total RNA within dry-stored seeds or aged seeds can be estimated by RNA integrity number (RIN) and this integrity is positively correlated to the potentiality of germination present within seeds (Fleming et al., 2017). Hence, mRNA could be a possible sensitive marker for aging (Fleming et al., 2018). RNA being a more fragile molecule than DNA, are easily damaged in stored seeds. Nucleobases in RNA can be easily converted to abasic sites or modified. mRNA strand

back bone is easily vulnerable to truncation during storage (Wurtmann and Wolin, 2010).

Usually in dry seeds mRNA are stable until the commencement of germination (Dure and Waters, 1965). But if seed storage periods are extended then the mRNA within seeds undergo oxidative attack. Loss of mRNA is brought about by deadenylation followed by decapping and loss of activity of enzymes like 5′–3′exonuclease or 3′–5′ exonuclease (Zhang and Guo, 2017).

DNA and RNA fragmentation, shortening of telomeres and particularly laddering have been associated with aging of seeds (Boubriak et al., 2007; Kranner et al., 2011).

This chapter looks at the effect of storage on the size, structure and integrity of the oil bodies. There are very few molecular studies on effect of aging on oleosins in seeds of natural or artificially aged oil seeds.

7.2. RESULTS

7.2.1. Staining of oil body and studying its structure

Microscopic studies of the oil bodies present within the seeds of *Jatropha curcas* show that the control seeds exhibit distinctive oil bodies within the cell and are characterized by increased numbers, uniformity in size and equal distribution within cytoplasm. No sign of fusion or coalescence or shrinking or damage of oil bodies was seen in control seeds. Oil bodies within cytoplasm are very prominent with circular or ovoid shape (Figure 7.2.1). This observation was true for all the seeds subjected up to 12 months of natural aging (Figures 7.2.1 and 7.2.2). As the natural aging is extended beyond 12 months, commencement of reduction in individual size and distortion in circular or ovoid shape of the oil bodies is marked. This damaged and distorted oil bodies is characteristic of all the seeds aged for 15 to 24 months of natural aging (Figures 7.2.2 and 7.2.3). Oil body features observed in AA12h, AA1d, AA2d and AA3d (Figures 7.2.4 and 7.2.5), and SSAA12h, SSAA1d, SSAA2d and SSAA3d (Figures 7.2.7 and 7.2.8) were more or less similar to those features of oil bodies observed in NA1m to NA12m. In extreme conditions like accelerated aging and saturated salt accelerated aging similar kind of detrimental effect is evident from AA4d

to AA7d (Figures 7.2.5 and 7.2.6) and from SSAA5d to SSAA7d (Figures 7.2.8 and 7.2.9). As accelerated aging and saturated salt accelerate aging progressed to the seventh day, there is more intense distorted shape of oil bodies and severely damaged unevenly distributed oil bodies. Significantly reduced number of oil bodies in seeds of AA and SSAA compared to control is obvious negative resultant effect of artificial aging. At this stage, loss of uniformity of shape in oil bodies, disorderly distribution of oil bodies within cytoplasm and shrinkage were clearly apparent.

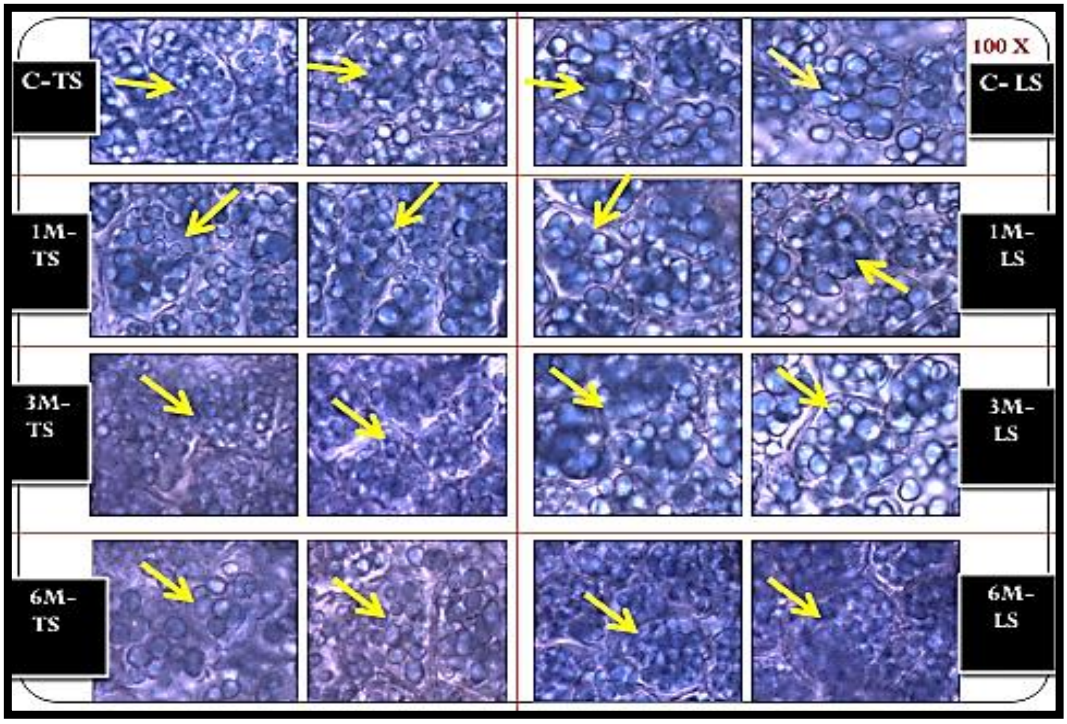

Figure 7.2.1: Staining of oil bodies by Sudan Black- B and images by light microscopy. TS – Transverse Section; LS – Longitudinal Section; C - control; 1M – NA1m; 3M – NA3m; 6M – NA6m.

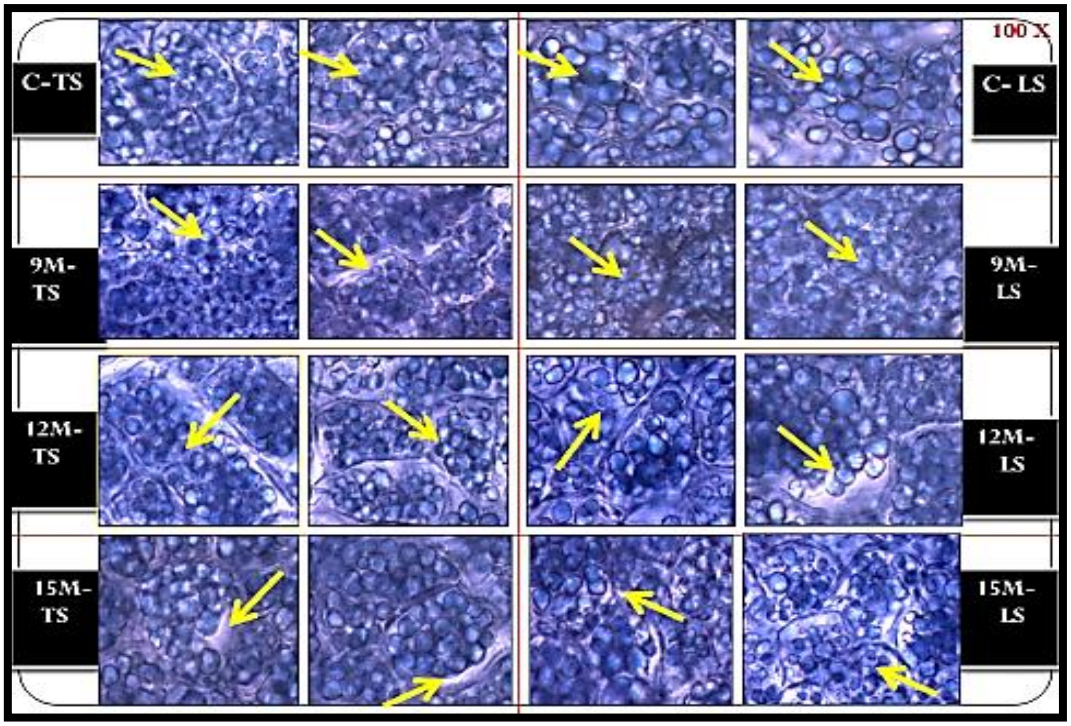

Figure 7.2.2: Staining of oil bodies by Sudan Black - B and images by light microscopy. TS – Transverse Section; LS – Longitudinal Section; C – control; 9M – NA9m; 12M – NA12m; 15M - NA15m.

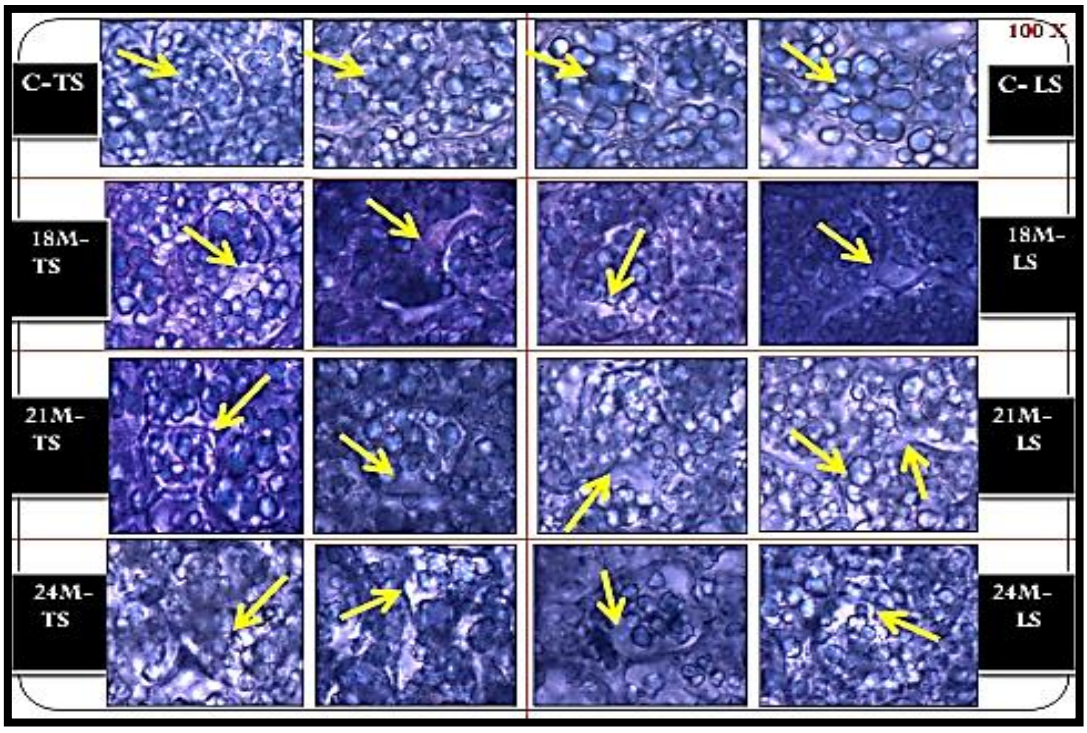

Figure 7.2.3: Staining of oil bodies by Sudan Black- B and images by light microscopy. TS – Transverse Section; LS – Longitudinal Section; C - control; 18M - NA18m; 21M - NA21m; 24M - NA24m.

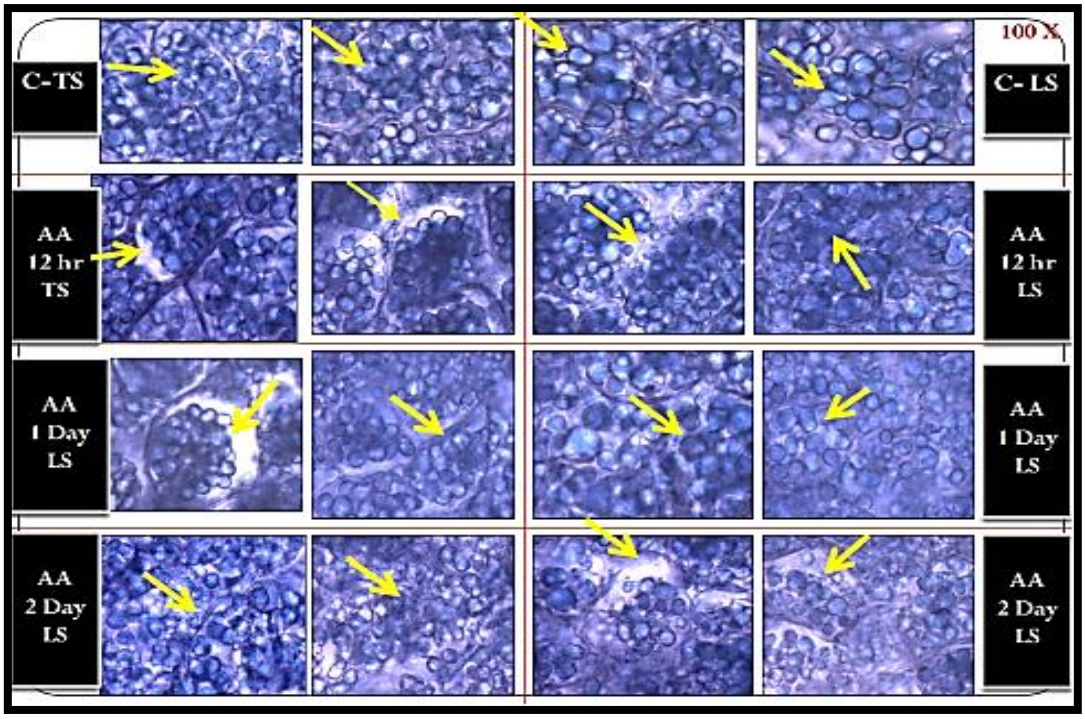

Figure 7.2.4: Staining of oil bodies by Sudan Black- B and images by light microscopy. TS – Transverse Section; LS – Longitudinal Section; C – control; AA12h; AA1d; AA2d.

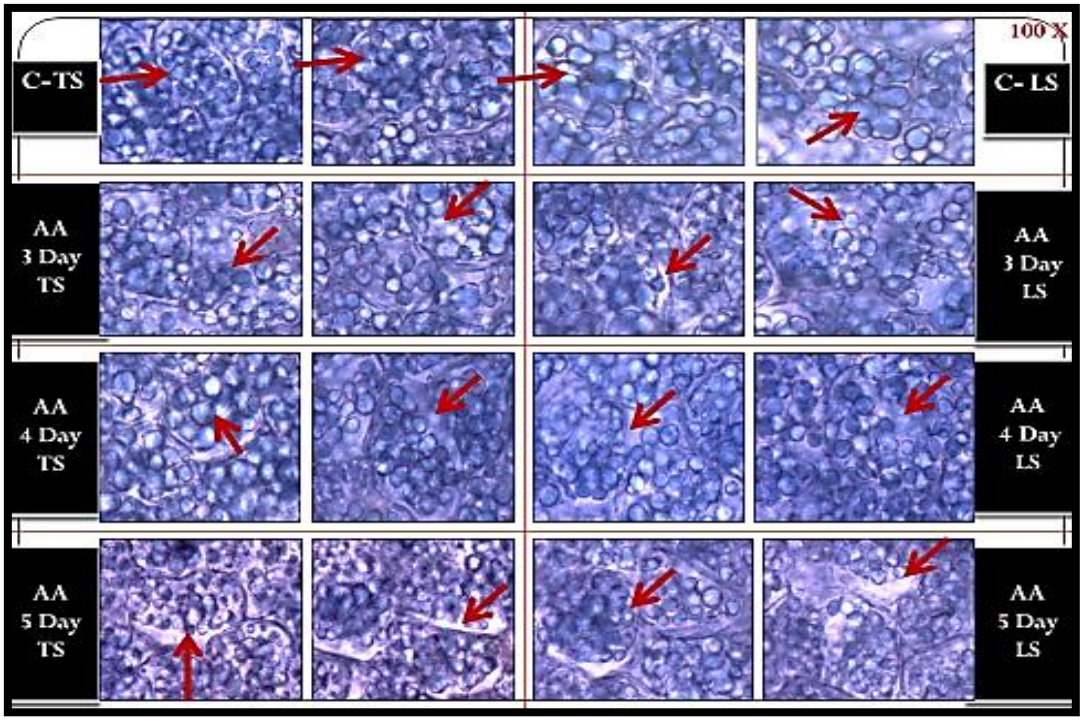

Figure 7.2.5: Staining of oil bodies by Sudan Black- B and images by light microscopy. TS – Transverse Section; LS – Longitudinal Section; C- control; AA3d; AA4d; AA5d.

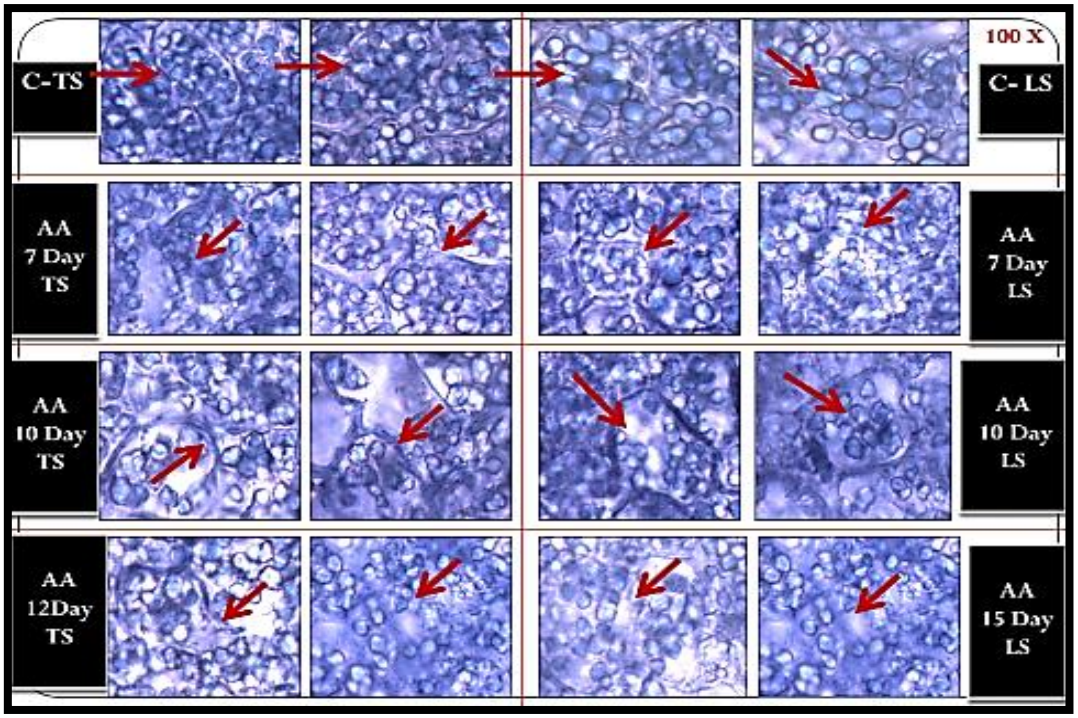

Figure 7.2.6: Staining of oil bodies by Sudan Black- B and images by light microscopy. TS – Transverse Section; LS – Longitudinal Section; C – control; AA7d; AA10d; AA12d; AA15d.

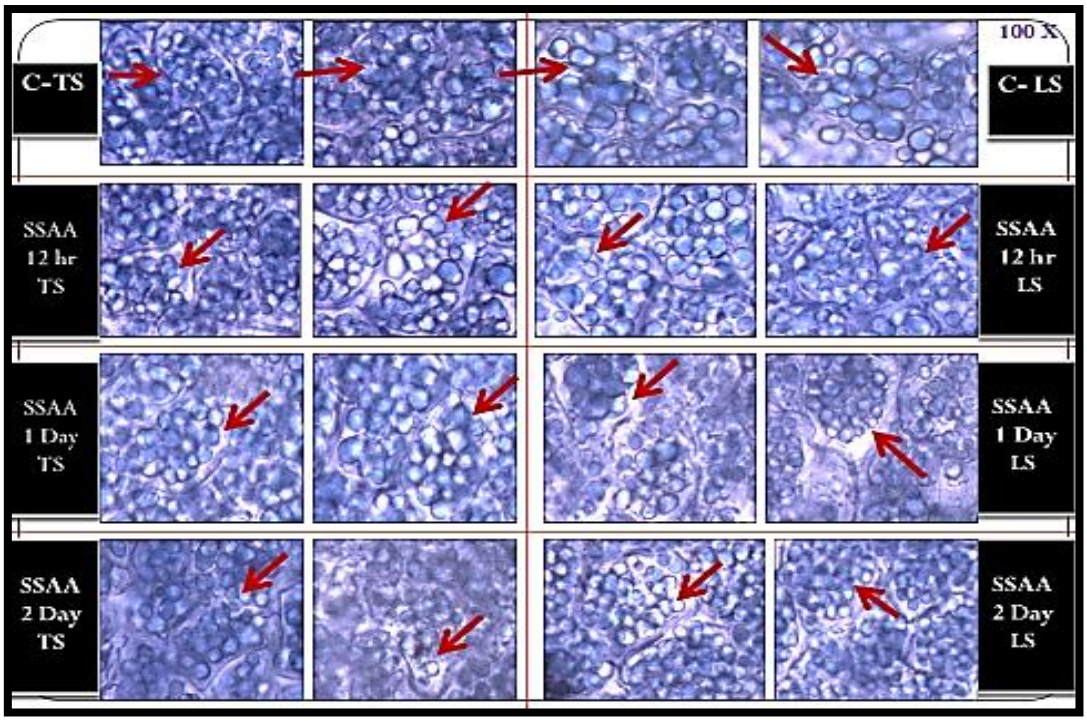

Figure 7.2.7: Staining of oil bodies by Sudan Black- B and images by light microscopy. TS – Transverse Section; LS – Longitudinal Section; C- control; SSAA12hr; SSAA1d; SSAA2d.

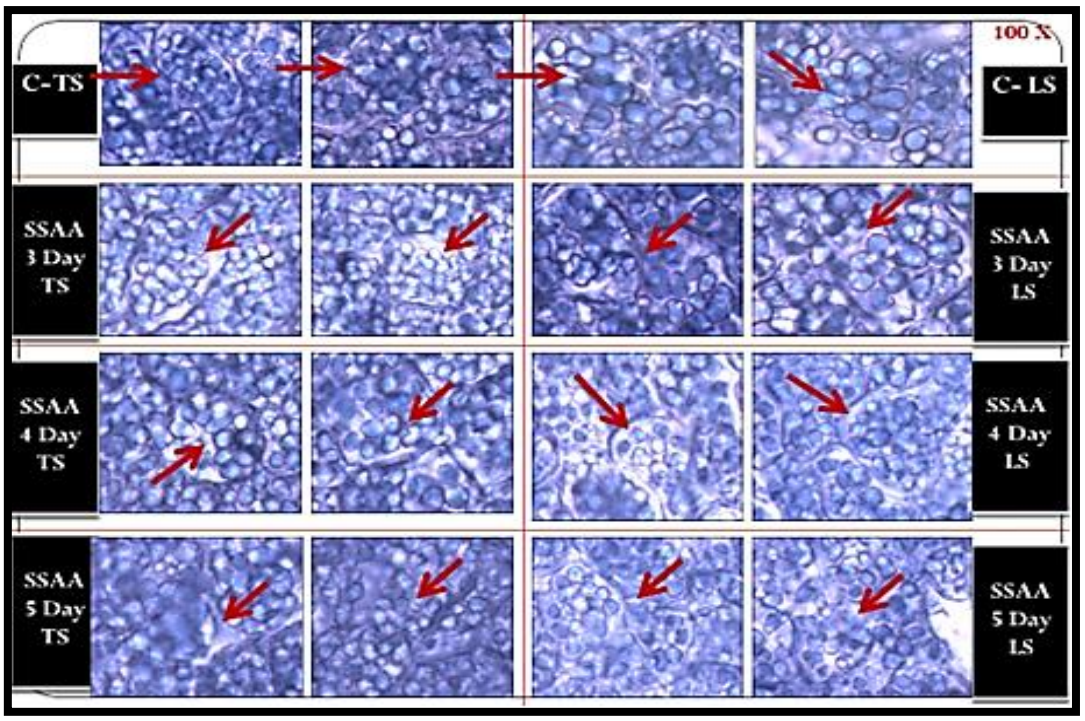

Figure 7.2.8: Staining of oil bodies by Sudan Black- B and images by light microscopy. TS – Transverse Section; LS – Longitudinal Section; C – control; SSAA3d; SSAA4d; SAA5d.

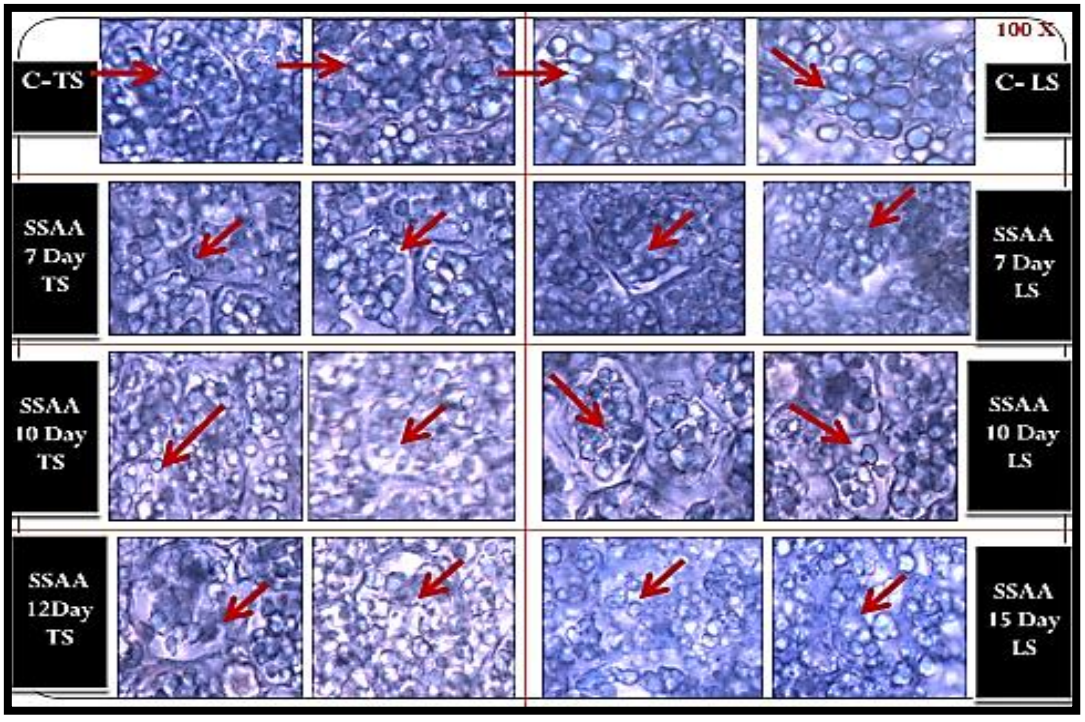

Figure 7.2.9: Staining of oil bodies by Sudan Black- B and images by light microscopy. TS – Transverse Section; LS – Longitudinal Section; C- control; SSAA7d; SSAA10d; SSAA12d; SSAA15d.

7.2.2. Studies on oil body specific protein – oleosins

Growing popularity of *J. curcas* as a source of biodiesel lead Popluechai et al., (2011) to isolate and characterize the major proteins of oil bodies, oleosins from *J. curcas* seeds. A chloroform/methanol ratio (11/7, *v/v*) as solvent in extraction process resulted in the best yield. Using *Arabidopsis* oleosin S2 antibodies (anti-rS2N) immune assays were conducted on total seed proteins. A cross-reactivity was observed with anti-rS2N antibody with an appearance of bands around 13 kDa and 26 kDa potentially corresponding to monomeric and dimeric forms of *J. curcas* oleosins was seen by Popluechai et al., in 2011 (Figure 7.3).

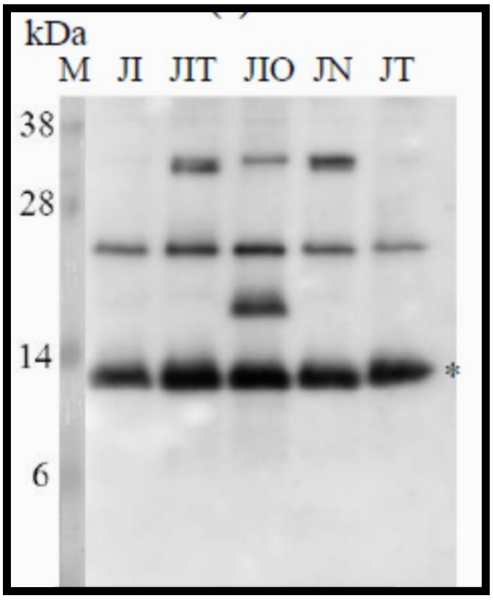

Figure 7.3: Immunological detection of oleosins using antiserum raised against *A. thaliana* oleosin S2 (anti rS2N). Total seed protein of *J. curcas* extracted from accessions belonging to India (JI and JIT), Indonesia (JIO), Nigeria (JN) and Thailand (JT) (**Popluechai et al., 2011**).

Using the method of Popluechai et al., (2011) (chapter 2), the extraction and isolation of oil body specific oleosin proteins was carried out successfully in the present study. Extracted crude proteins from control seeds showed a presence of 26 kDa prominent oleosin protein band along with other bands indicating the presence of other oil body associated membrane bound proteins (Figure 7.3.1). The seeds subjected to natural aging showed similar results with the occurrence of a band at 26 kDa indicating the presence of oleosin (Figure 7.3.2). Densitometry analysis showed that the intensity

of the band has significantly reduced from 15th month of natural aging (Figure 7.3.5). Seeds that were subjected to 12 hours to five days of both accelerated and saturated salt accelerated aging also expressed similar kind of band at 26 kDa but there was total absence of such band from seventh day of AA and SSAA (Figures 7.3.3 and 7.3.4). Intensity of the band gets significantly reduced from AA1d and SSAA2d onwards (Figures 7.3.6 and 7.3.7).

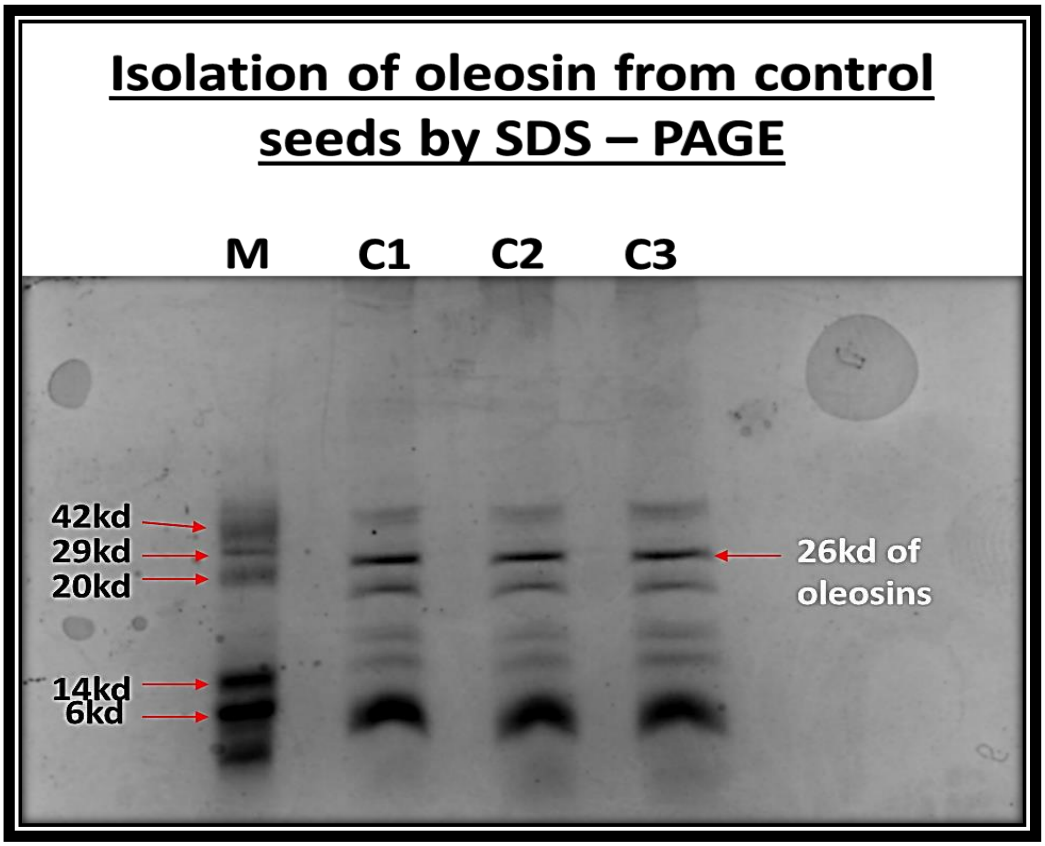

Figure 7.3.1. SDS-PAGE for oleosin obtained from control seeds (NA), n=3. M – marker **and C – control.**

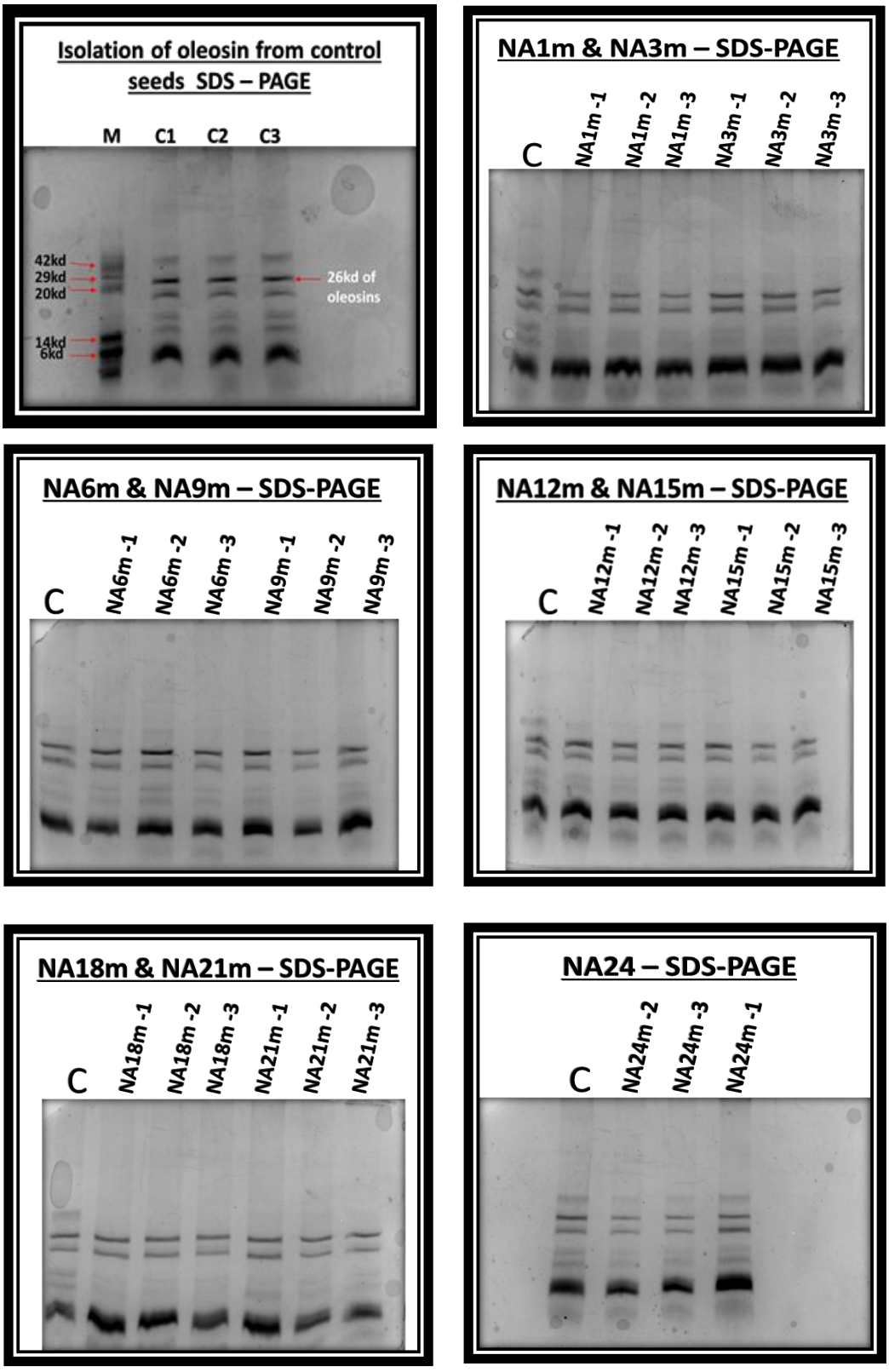

Figure 7.3.2. SDS-PAGE for oleosin obtained from control seeds and seeds of natural aging (NA), n=3.

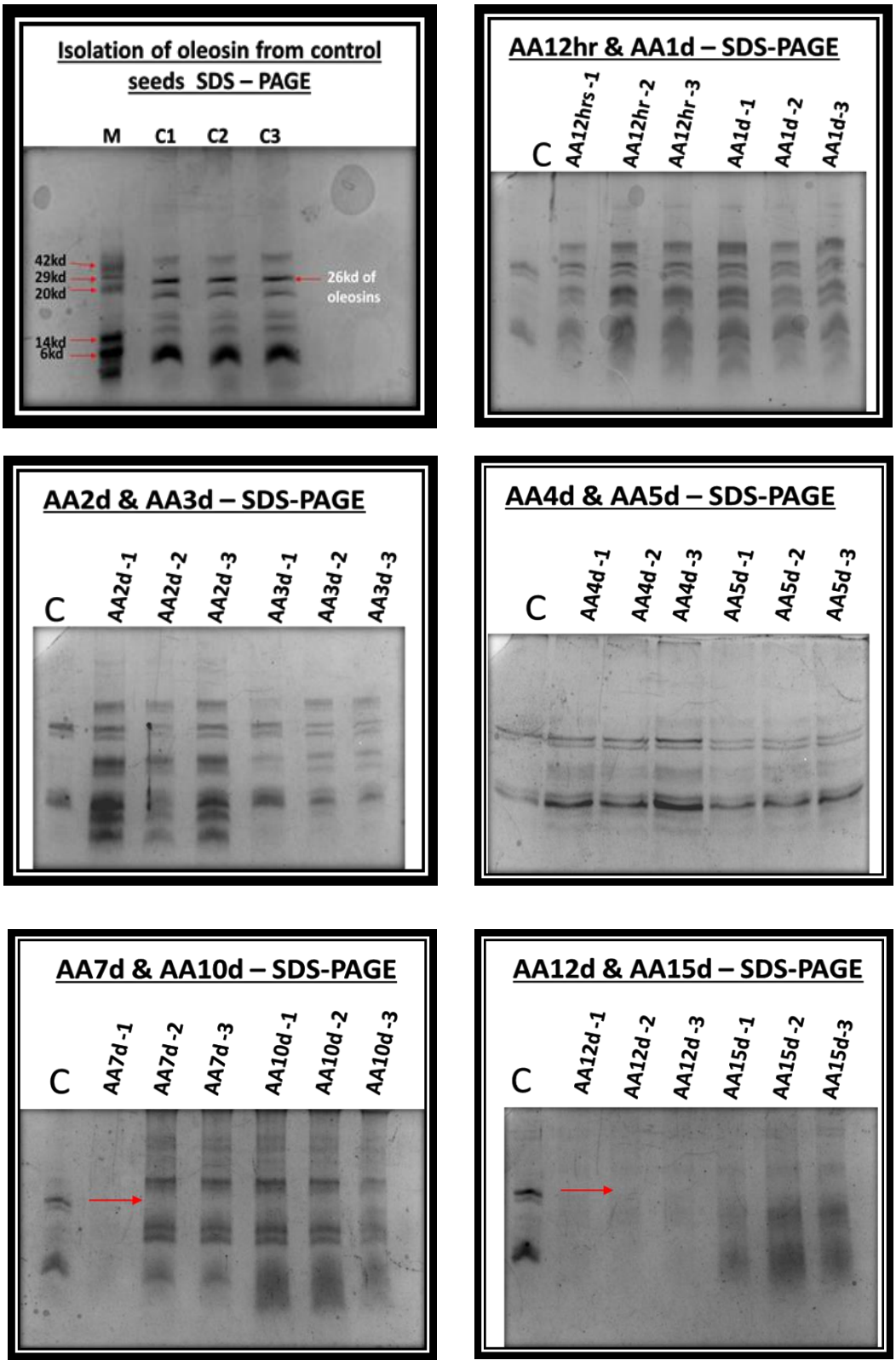

Figure 7.3.3. SDS-PAGE for oleosin obtained from control seeds and seeds of accelerated aging (AA), n=3.

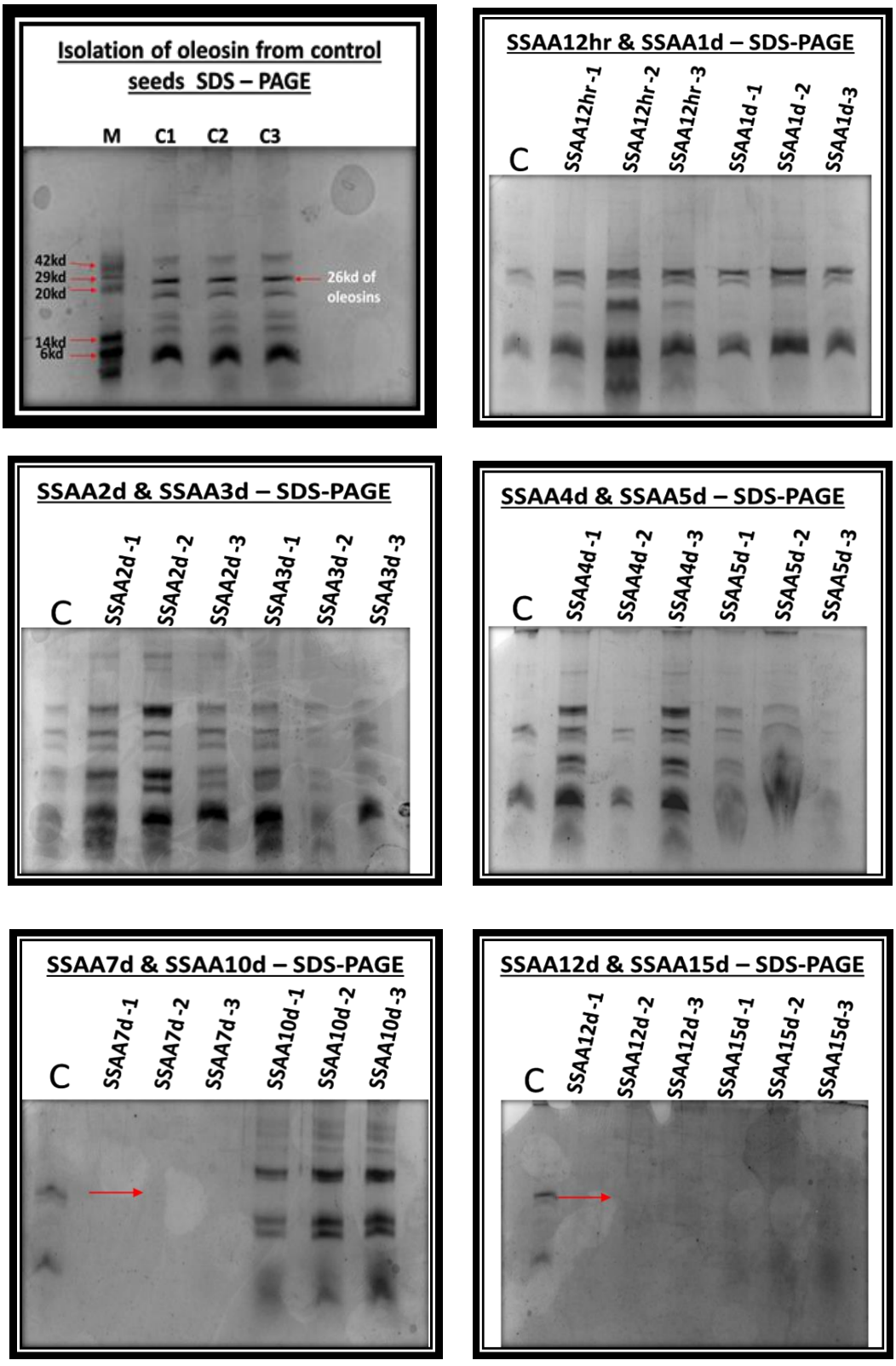

Figure 7.3.4 SDS-PAGE for oleosin obtained from control seeds and seeds of saturated salt accelerated aging (SSAA), n=3.

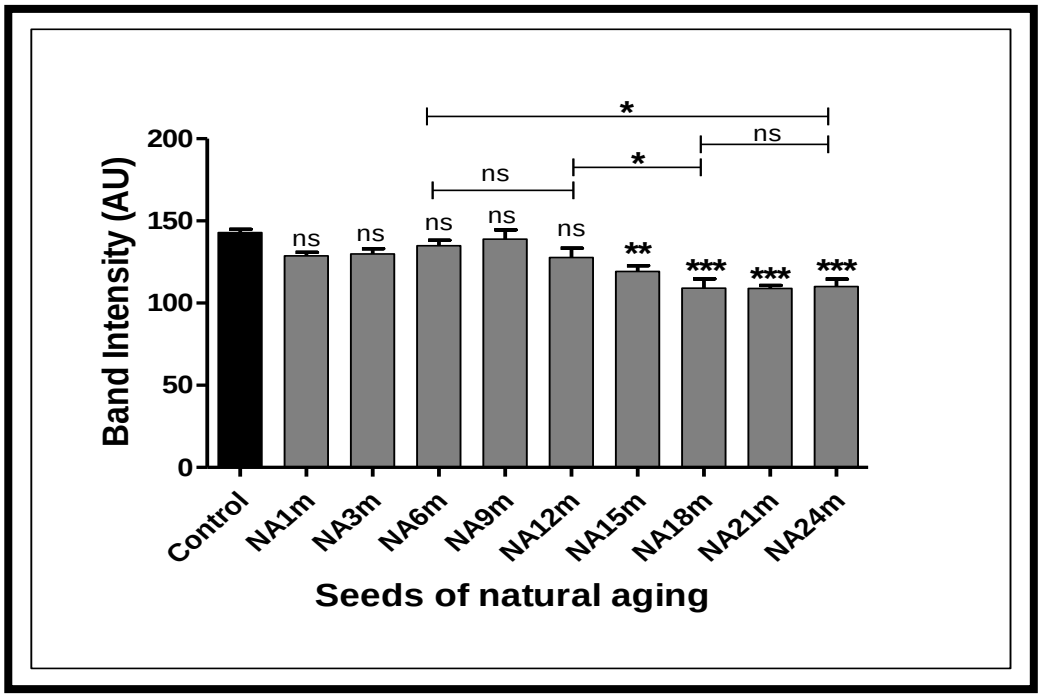

Figure 7.3.5. Analysis of band intensity of oleosin extracted from seeds of natural aging (NA), n = 3.

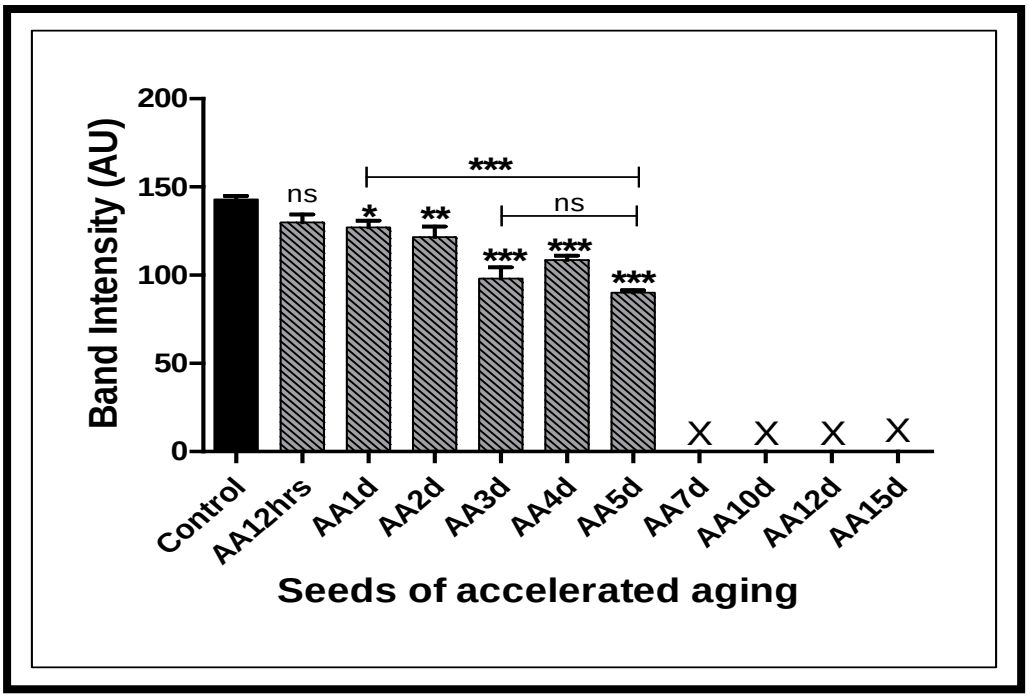

Figure 7.3.6: Analysis of band intensity of oleosin extracted from seeds of accelerated aging (AA), n = 3.

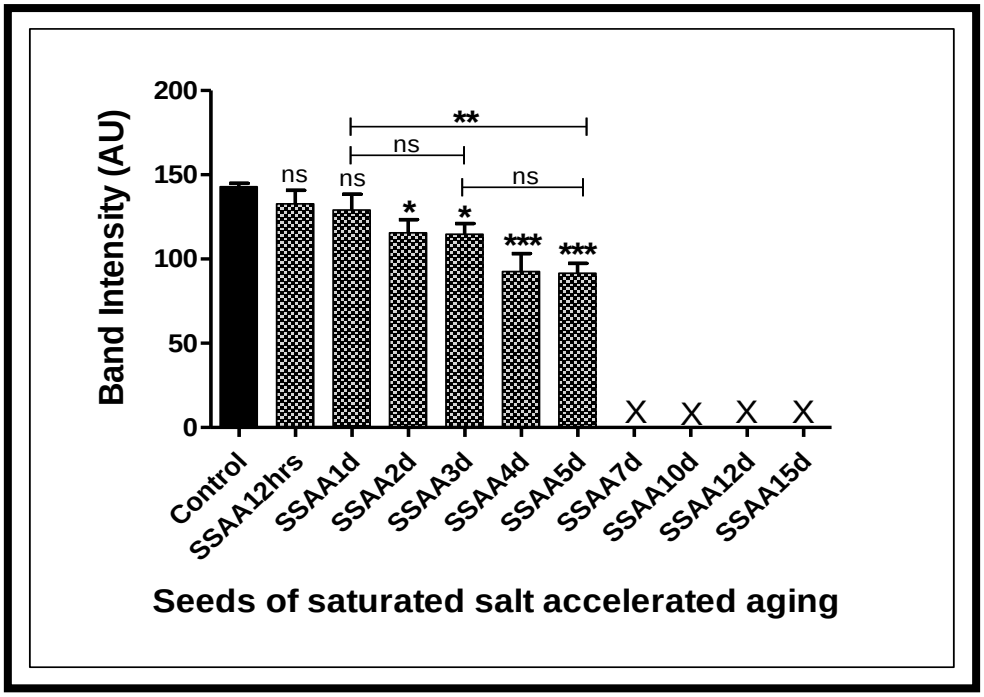

Figure 7.3.7: Analysis of band intensity of oleosin extracted from seeds of saturated salt accelerated aging (SSAA), n = 3.

7.2.3. Extraction and isolation of genomic DNA of *J. curcas*

Genomic DNA of *J. curcas* was extracted and isolated from seeds by the method of Doyle and Doyle (1990) as described in chapter 2 to analyse the effect of aging at genomic level. DNA could successfully be extracted and a prominent band was observed on electrophoresis for samples from control seeds, NA6m and NA12m (Figure 7.4. A). Smearing of the band was observed for DNA samples extracted from seeds aged beyond 15m (Figure 7.4. A). With respect to artificial aging, DNA samples extracted from AA1d, AA3d, SSAA1d and SSAA3d showed no loss of DNA integrity and a prominent DNA band was seen (Figure 7.4. B). Smearing was observed in DNA sample extracted from AA5d onwards (Figure 7.4. B). Using the protocol mentioned, no DNA was detected in the sample extracted from SSAA5d (Figure 7.4. B). Intensity of the band was also low in SSAA1d and SSAA3d. Since smearing effect of the band in AA5d and absence of band in SSAA5d was already observed, DNA analysis was not done in seeds subjected to longer periods of aging.

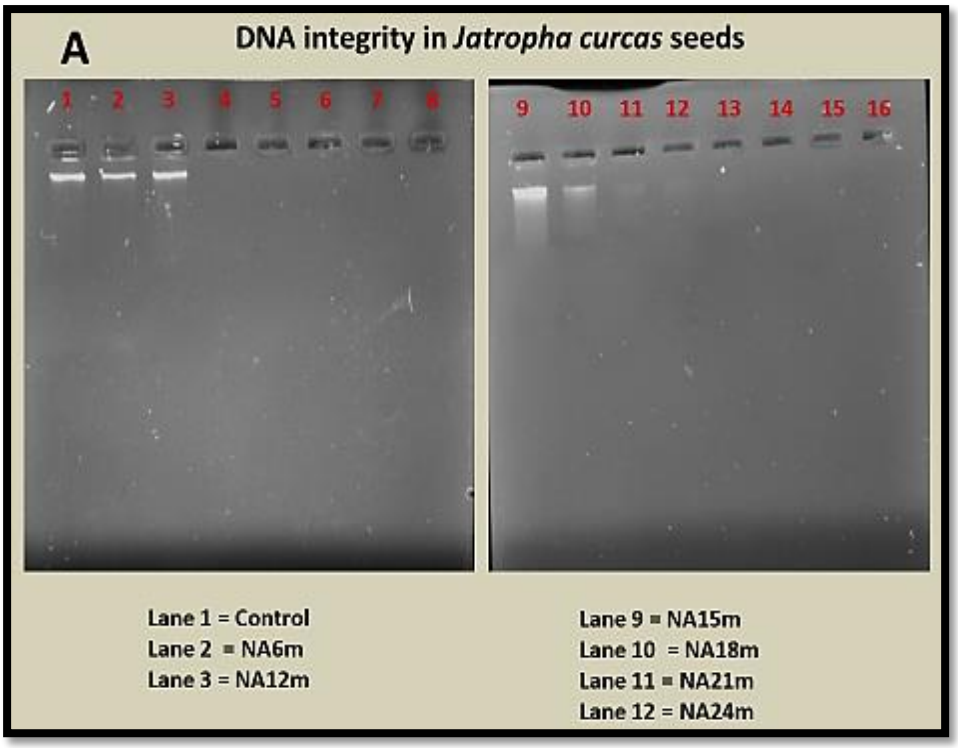

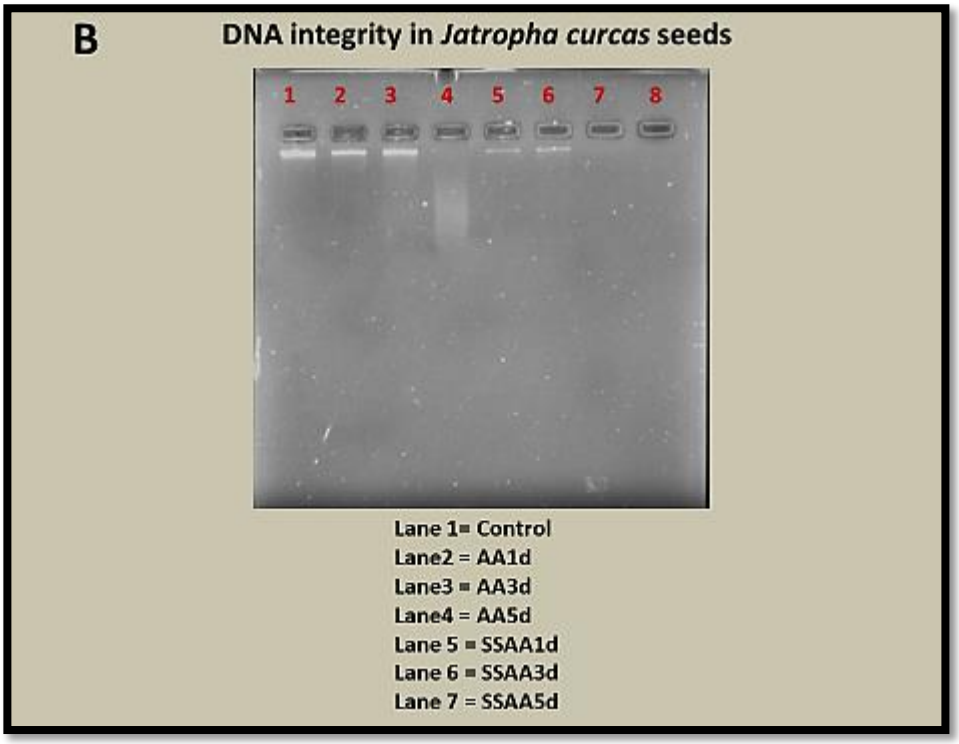

Figure 7.4: Extraction and isolation of genomic DNA from *J. curcas* seeds. A – Natural aging; B – Accelerated and saturated salt accelerated aging.

7.2.4. Studies on nuclear morphology by DAPI staining

Nuclear morphology of cells in the seed tissue was studied by using DAPI dye. As per the protocol of El-Maarouf-Bouteau et al., (2011) (chapter 2), the cells were stained by DAPI dye and observed under Bright field microscopy with 40X magnification first and then the same field was observed under fluorescence lamp. Microscopic studies reveal that in control seeds the cells that underwent staining by DAPI and expressed fluorescence were more in number compared to all the other groups of seeds. Cells appeared distinct, oval/round in shape (Figure 7.5 A). Similar observation was found in tissues of seeds of NA1m, NA3m, NA6m and NA9m. As natural aging was prolonged the stained cells were gradually decreased in tissues of seeds from NA12m onwards (Figure 7.5 A). Similar kind of gradual decrease of stained cells were also evident in tissues of seeds of accelerated and saturated salt accelerated aging (Figures 7.5 B and 7.5 C). As the artificial aging treatment was increased cells that underwent DAPI staining were extremely meagre.

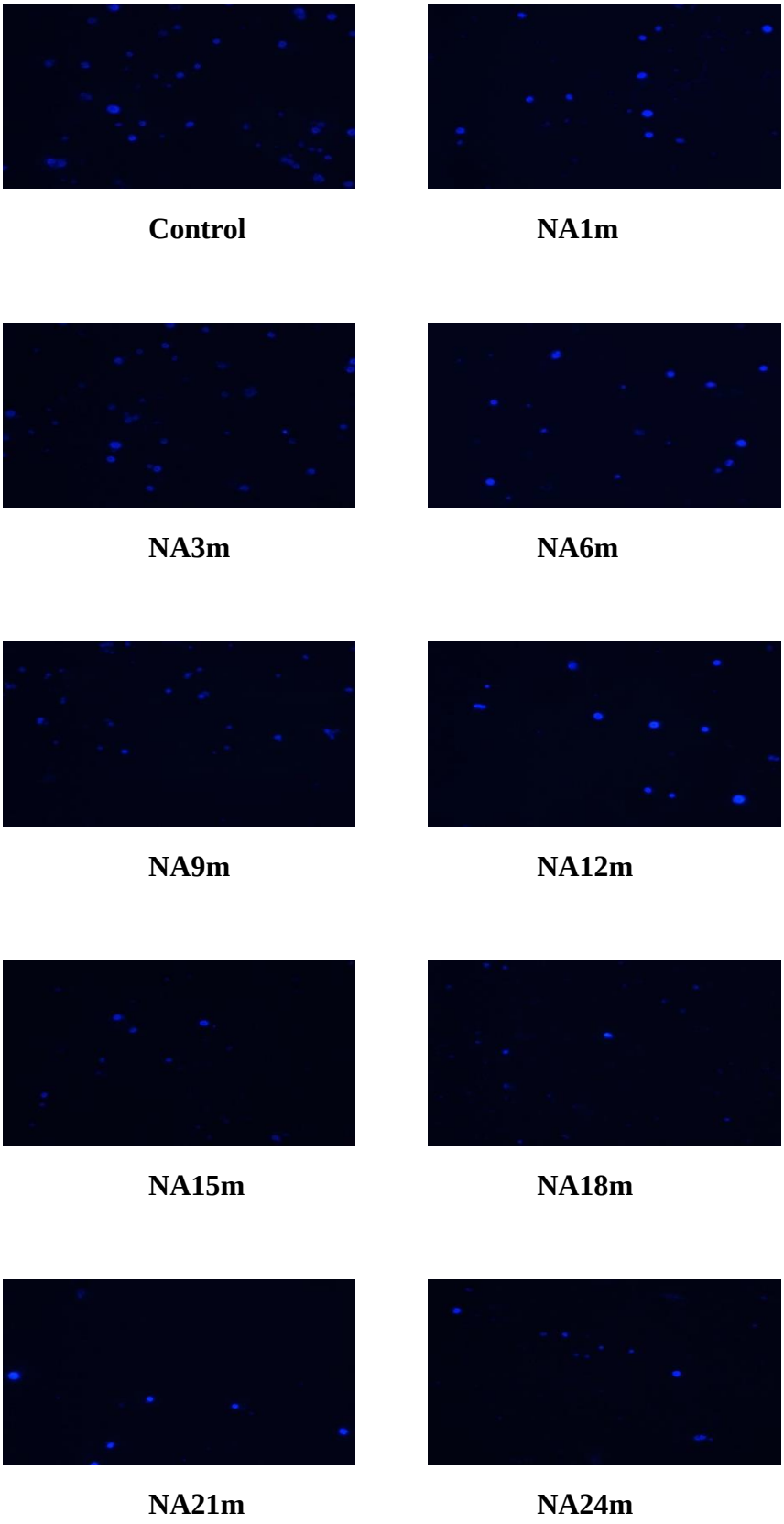

Figure 7. 5 A: DAPI staining of control seeds and seeds of natural aging of *J. curcas*.

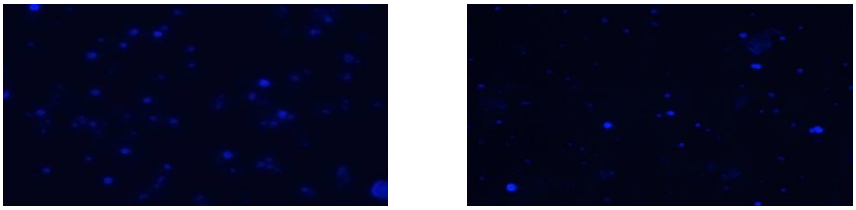

AA12hr **AA1d**

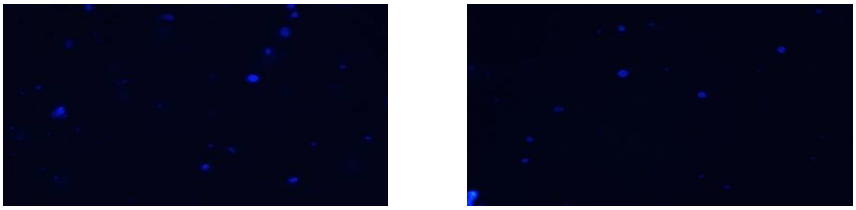

AA2d **AA3d**

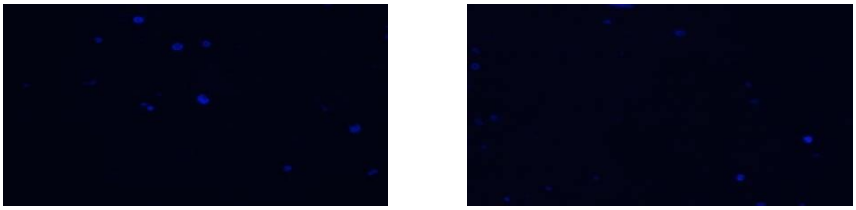

AA4d **AA5d**

AA7d **AA10d**

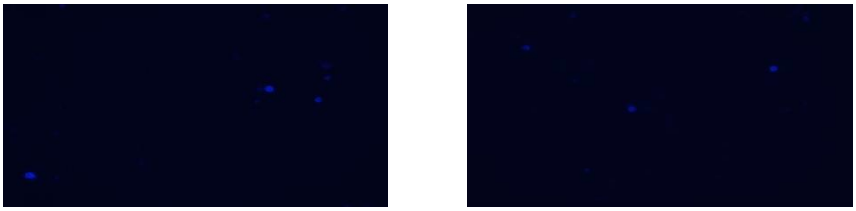

AA12d **AA15d**

Figure 7. 5 B: DAPI staining of seeds of accelerated aging of *J. curcas*.

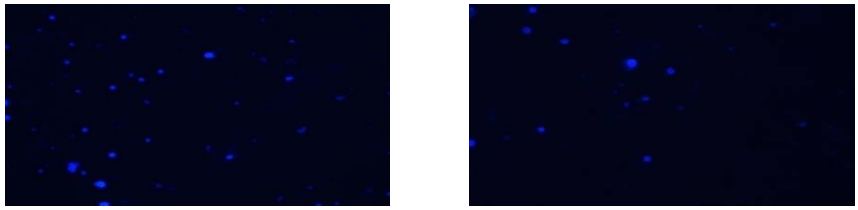

SSAA12hr **SSAA1d**

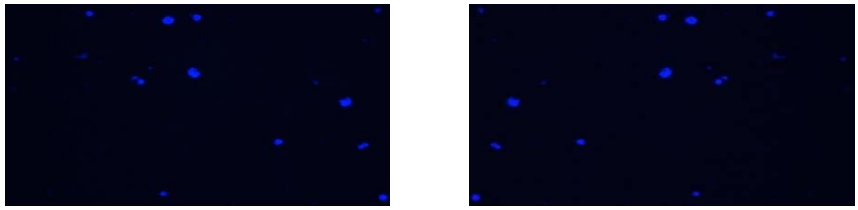

SSAA2d **SSAA 3d**

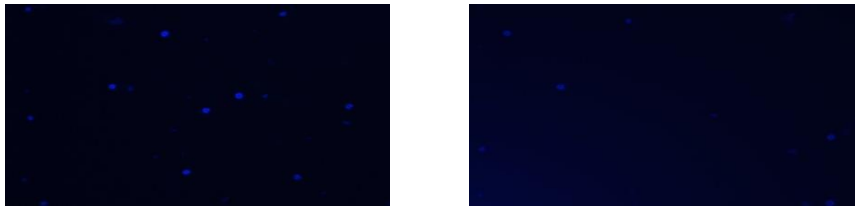

SSAA4d **SSAA5d**

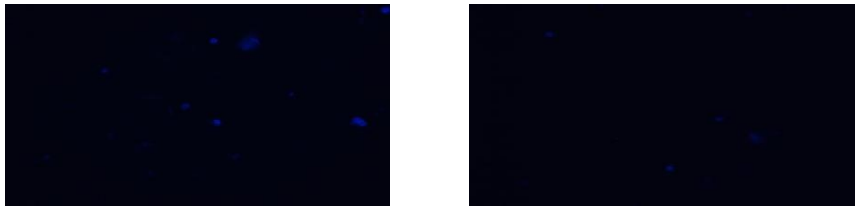

SSAA7d **SSAA10d**

SSAA12d **SSAA15d**

Figure 7. 5 C: DAPI staining of seeds of saturated salt accelerated aging of *J. curcas.*

7.3. DISCUSSION

7.3.1. Studies on oil body staining and structure

Loss in DNA integrity and content can be attributed to the negative destructive effect on oil bodies during storage and accelerated aging due to lipid peroxidation of TAG which results in marked upheaval in MDA, H_2O_2, and increased level of free fatty acids and reduction of oil content. The free radicles formed as a result of these changes are the sinister molecules that bring about membrane disruption of the oil bodies leading to reduction and distortion of the oil bodies. Results of the present study are in conformity with the earlier studies done on *Arabidopsis thaliana* where seeds on storage showed membrane degradation, fusion of oil bodies, and reduction of size and shape of oil bodies (Shimada et al., 2008). Oleosins - amphipathic proteins in oil bodies of seeds play a pivotal and significant role in stabilizing of oil bodies and preventing coalescence of oil bodies during desiccation (Popluechai, 2011). The stability of oil bodies is the consequence of the steric hindrance and electrostatic repulsion provided by oleosins on their surfaces (Tzen et al., 2012). In this study, it was observed that those seeds that maintain the optimum level of oleosin during storage or artificial aging had the ability to preserve the stability and shape of oil bodies. Seeds that could not uphold optimum oleosin level succumbe to oil body damage.

7.3.2. Studies on oil body protein - oleosin

SDS-PAGE followed by densitometry analysis of bands confirms the denaturation of oleosins. Significant loss of band intensity from NA15m onwards in natural aged seeds and from AA1d and SSAA2d onwards in artificially aged seeds clearly depicts the reduction of oleosins and their denaturation due to prolonged period of natural aging and artificial aging. Complete loss of oleosin seen from AA7d and SSAA7d onwards. According to Siloto et al., (2006) and Ting et al., (1996) there is a correlation between oleosin levels and oil body size in oil seeds. Species that express higher amount of oleosins contain smaller size of oil bodies. Similarly, species with lower amount of oleosins have larger size of oil bodies (Hu et al., 2009). Large number of smaller size-oil bodies observed through light microscopy confirms the presence of higher amount of oleosin in seeds of *J. curcas* in the present study (Section 7.2.1). With respect to natural aging, significant reduction in the band intensity of oleosin is manifested through the distortion and reduction of size and shape of oil bodies in these

groups of seeds of NA15m to NA24m. Similar observation can be made for AA4, AA5d, SSAA4d and SSAA5d. Complete absence of the band indicates total absence of oleosin and this is reflected in total distortion and damage occurring to oil bodies in the seeds of AA7d to AA15d and SSAA7d to SSAA15d (Figure 7.2.6 and 7.2.9). Hence damage to oil bodies, loss of stability in oil bodies, reduced number of oil bodies and distortion of oil bodies seen in NA15m to NA24m, AA5d to AA15d and SSAA5d to SSAA15d can be attributed to loss of oleosin as they are denatured or destroyed during prolonged period of storage and extreme condition of temperature and moisture. Even though oleosins do not play an important role in lipid body biogenesis still it plays a key role in post-germinative rehydration of seeds (Leprince et al., 1998). Emergence of radical observed during germination in control seeds, in NA1m to NA12m, inAA12h to AA3d and in SSAA12h to SSAA3d confirms this post-germinative key role of oleosin in these groups of seeds. Absence of emergence of radicals found in older groups of seeds affirms the impairment of oleosins due to reduction or complete loss of oleosin during storage.

7.3.3. Studies on genomic DNA of *J. curcas* seeds on storage.

Aging is a common phenomenon in all the living entities and as a result of aging, a progressive decline in all the vital events occur culminating to death at the end. An elevated level of moisture content and temperature is lethal to cells. Macromolecules including DNA are the ultimate target of the OH* radicals, leading to degradation of cellular components and eventually to cell death (Hu et al., 2012). The effect of seed aging on quantity and quality of DNA was studied in the present investigations. There is good correlation between viability loss and chromosome damage in seeds, over a fairly wide range of temperatures and moisture content (Roberts, 1973). DNA cleavage is considered to be one of early events of programmed cell death. The random cleavage of DNA as a result of DNase activity occurs in the dry seed. In our study loss of DNA integrity was not found in natural aging up to 12 months. The smearing effect seen in NA15m to NA24m, and AA5d indicates a loss of DNA integrity/DNA damage. Similar results were reported in beech seeds (Ratajczak, 2015) and maize seed (Radha et al., 2014) where decrease in total DNA content and loss of DNA integrity was observed as aging prolonged. Integrity of macromolecules such as DNA is not maintained during seed ageing (Radha et al., 2014). As seeds lose viability during ageing, DNA was gradually degraded into inter nucleosomal fragments,

resulting in ―DNA laddering. A clear sign of DNA fragmentation seen through DNA laddering was observed in beech seeds stored for 5 years (Ratajczak, 2015). Gel electrophoresis in the present study did not show DNA laddering but showed DNA smearing. Accumulation of ROS can be considered to be part of the signalling molecules in bringing about the cascade of reactions culminating in programmed cell death (Vacca et al., 2004, El-Maarouf-Bouteau et al., 2011). Previously reported studies on pea seeds during accelerated aging (Kranner et al., 2011), sunflower seeds during storage (El-Maarouf-Bouteau et al., 2011) and elm seeds during controlled deterioration (Hu et al., 2012) confirm DNA laddering, as related to plant PCD.

7.3.4. Studies on nuclear morphology of cells by DAPI staining.

Double stranded DNA reversibly binds to a water-soluble blue fluorescent dye known as DAPI (4′, 6-diamidino-2-phenylindole) (Huschka et al., 2010). DAPI binds to the minor grooves of double stranded DNA. Quantum yield gets increased when DAPI and dsDNA associate with each other (Barcellona and Gratton, 1990).

Our results revealed that cells showed fluorescence in the control and naturally aged seeds up to 12 months. This indicates binding of the dye to the double standard DNA confirming the chromosomal integrity in the control seeds and as well as in the seeds of natural aging up to 12 months. This is to say that almost no or less nuclear damage, dispersion of nuclei and nuclei membrane in these groups of seeds. As the seeds were subjected to accelerated aging the same kind of result like that of control was observed up to 2 days of accelerated aging and 3 days of saturated salt accelerated aging. This corresponds with the results from the studies on DNA integrity by gel electrophoresis, where a presence of clear distinct DNA band in control seeds, NA6m, NA12m, AA1d, SSAA1d, and SSAA3d is seen which on aging results to a smear on gel. With increase in age of seeds beyond 12 months of natural aging, and accelerated aging treatment above 1 or 2 days and saturated salt accelerated aging above 3 days resulted in fluorescence of particles in a scattered manner and also prominent distinct oval or round shaped fluorescence appeared less in number compared to control. This may indicate possible chromosomal-DNA disintegration due to the abnormal conditions of prolonged storage and artificial aging. As the accelerated aging progresses there is an increased DNA damage, dispersion of nuclei and nuclear membrane compare to control. This kind of nuclear damage may indicate a necrotic type of cell death found in AA3d to AA15d, and SSAA4 to SSAA15d. However, this results need to be further

confirmed through Propidium Iodide (PI) staining for dead cells. Oxidative stress and lipid peroxidation have been widely indicated as the major cause of deterioration of oil seeds during aging (McDonald et al., 1999).